Syntheses and Solid-State NMR of *n*-Bu_4NTeH, Me_4NSeH, and $(Me_4N)_2Te_2$ and X-ray Crystal Structures of Me_4NSeH and $(Me_4N)_2Te_2$

R. J. Batchelor, F. W. B. Einstein, I. D. Gay, C. H. W. Jones,* and R. D. Sharma

Department of Chemistry, Simon Fraser University, Burnaby, British Columbia, Canada V5A 1S6

*Received August 25, 1992**

The syntheses of *n*-Bu_4NTeH, Me_4NSeH, and $(Me_4N)_2Te_2$ are described. The compounds have been characterized by ^{123}Te, ^{125}Te, and ^{77}Se solid-state NMR spectroscopy and by ^{125}Te Mössbauer spectroscopy. The X-ray crystal structures of Me_4NSeH and $(Me_4N)_2Te_2$ are reported and some structural data for *n*-Bu_4NTeH are given. For Me_4NSeH: tetragonal space group $P4/nmm$, $Z = 2$, $a = 7.8855(8)$ Å, $c = 5.6484(5)$ Å, $V = 351.22$ Å^3, $R_F = 0.020$ for 180 data with $I_o \geq 2.5\sigma(I_o)$; isostructural with Me_4NBr. For $(Me_4N)_2Te_2$: cubic space group $Pa\bar{3}$, $Z = 4$, $a = 11.499(1)$ Å, $V = 1520.5$ Å^3, $R_F = 0.018$ for 454 data with $I_o \geq 2.5\sigma(I_o)$; the ionic packing is of the anti-fluorite type.

Introduction

As part of a continuing study of the Mössbauer and NMR spectroscopy and X-ray crystallography of compounds of tellurium, we have investigated the TeH^- and Te_2^{2-} ions.[1] Initially, we studied the products of the reaction of potassium with tellurium in ethylenediamine. The ^{125}Te solution NMR spectra of the TeH^- and Te_x^{2-} anions ($x = 2$–4) showed the presence of rapid exchange. Recently Bjorgvinsson and Schrobilgen[2] reported a detailed and elegant NMR study of solutions of the tellurium, selenium, and tellurium/selenium polyanions in ethylenediamine and liquid ammonia and were able to characterize the solution NMR parameters of Te^{2-}, TeH^-, Te_2^{2-}, and Te_3^{2-}.

As a second route to the preparation of the tellurium anions, we explored the use of MBH_4 (M = Na, Me_4N, Et_4N, *n*-Bu_4N) as the reducing agent and have been able to prepare and identify recrystallizable compounds containing the TeH^-, SeH^-, and Te_2^{2-} anions. These compounds have been characterized by ^{123}Te, ^{125}Te, and ^{77}Se solid-state NMR spectroscopy and by X-ray crystallography, and by ^{125}Te Mössbauer spectroscopy for the tellurium anions. These studies complement the ^{125}Te and ^{77}Se NMR investigations by Bjorgvinsson and Schrobilgen[2] and by Cusick and Dance,[3] which were published while the present work was in progress. An X-ray crystal structure of Ph_4PTeH has been reported by Huffman and Haushalter.[4] Until very recently, the only structural data available for the Te_2^{2-} ion were an X-ray powder study of $MgTe_2$,[5] a neutron diffraction investigation of $MnTe_2$,[6] and a Te–Te bond length for α-K_2Te_2 reported in ref 7. The single-crystal structure of β-K_2Te_2 has now also been reported.[8]

Results and Discussion

Preparation of Solutions of the TeH^- and SeH^- Anions. Elemental tellurium reacts smoothly with a stoichiometric quantity of $NaBH_4$ in DMSO and a number of other solvents to give solutions containing the TeH^- ion. The ^{125}Te NMR spectrum of this ion in DMSO is characterized by a sharp, well-resolved doublet (Figure 1a) with $\delta = -919$ ppm and $^1J_{^{125}Te-^1H} = 160$ Hz. The proton-decoupled spectrum gave a broadened single line at −926 ppm, the difference in the chemical shift presumably arising from temperature effects. The ^1H NMR of a solution in DMSO-d_6 gave $\delta = -13.1$ ppm and $^1J_{^1H-^{125}Te} = 160$ Hz.

The present NMR data for TeH^- are in reasonable agreement with those of ref 2. In that work a weak doublet was observed at −1095 ppm ($^1J_{^{125}Te-^1H} = 140$ Hz) in the ^{125}Te spectra of solutions of K and Te in ethylenediamine containing 2,2,2-crypt. This doublet was also observed for the ethylenediamine (12-crown-4) solution extracts of $LiPbTe_{0.67}Se_{0.33}$ alloy. The proton NMR spectrum exhibited the coupling to ^{125}Te and gave a $\delta(^1H)$ of −12.9 ppm. The origin of TeH^- in these systems was not clear, and it was postulated that it arose from deprotonation of the solvent or the complexing ligand.

As noted above, the borohydride reduction could be carried out in a variety of solvents, and as shown in Table I, there appears to be a significant variation in the ^{125}Te chemical shifts in H_2O and in ethanol as compared with DMSO, DMF, or CH_3CN, possibly reflecting the effects of solvation of the TeH^- anion on the shielding, while the variation in $^1J_{^{125}Te-^1H}$ may reflect the presence of exchange with traces of Te_x^{2-} anions present in these solutions.

The SeH^- anion could also be produced in solution by reacting a borohydride with selenium. The ^{77}Se spectrum of a solution in methanol is shown in Figure 1b. The $^1J_{^{77}Se-^1H}$ coupling was not resolved in this spectrum. Cusick and Dance[3] have studied the ^{77}Se NMR of the SeH^- anion in a variety of solvents ($\delta = -447$ to −529 ppm) and observed the $^1J_{^{77}Se-^1H}$ coupling in aqueous (26 Hz) and ethanolic (25 Hz) solutions. In DMF/ethanol solutions a $^1J_{^{77}Se-^1H}$ coupling of only 16–19 Hz was observed in the presence of broadened line widths, and the presence of exchange between SeH^- and traces of Se^{2-} present in solution was proposed.

Preparation of *n*-Bu_4NTeH, Et_4NTeH, and Me_4NSeH. In characterizing the products of the reaction of BH_4^- with tellurium, we were interested in obtaining solids which could be investigated by Mössbauer spectroscopy and solid-state NMR, as well as by X-ray crystallography. The requirements for solid-state NMR suggested the use of the cations Me_4N^+, Et_4N^+, and *n*-Bu_4N^+. The reactions of Me_4NBH_4 with tellurium will be discussed separately below because they led to the isolation of the ditelluride $(Me_4N)_2Te_2$.

The reactions of Et_4NBH_4 and *n*-Bu_4NBH_4 with tellurium in DMF produced white solids which were soluble in, and could be

* Abstract published in *Advance ACS Abstracts*, August 15, 1993.

(1) Gay, I. D.; Jones, C. H. W.; Sharma, R. D. Paper presented at the Fifth International Conference on the Organic Chemistry of Selenium and Tellurium, Osaka, Japan, 1991.
(2) Bjorgvinsson, M.; Schrobilgen, G. J. *Inorg. Chem.* **1991**, *30*, 2540.
(3) Cusick, J.; Dance, I. *Polyhedron* **1991**, *10*, 2629.
(4) Huffman, J. C.; Haushalter, R. C. *Polyhedron* **1989**, *8*, 531.
(5) Yanagisawa, S.; Tashiro, M.; Anzai, S. *J. Inorg. Nucl. Chem.* **1969**, *31*, 943.
(6) Hastings, J. M.; Elliot, N.; Corliss, L. M. *Phys. Rev.* **1959**, *115*, 13.
(7) Ansari, A. A.; Ibers, J. A. *Coord. Chem. Rev.* **1990**, *100*, 223.
(8) Böttcher, P.; Getzschmann, J.; Keller, R. *Z. Anorg. Allg. Chem.* **1993**, *619*, 476.

0020-1669/93/1332-4378$04.00/0

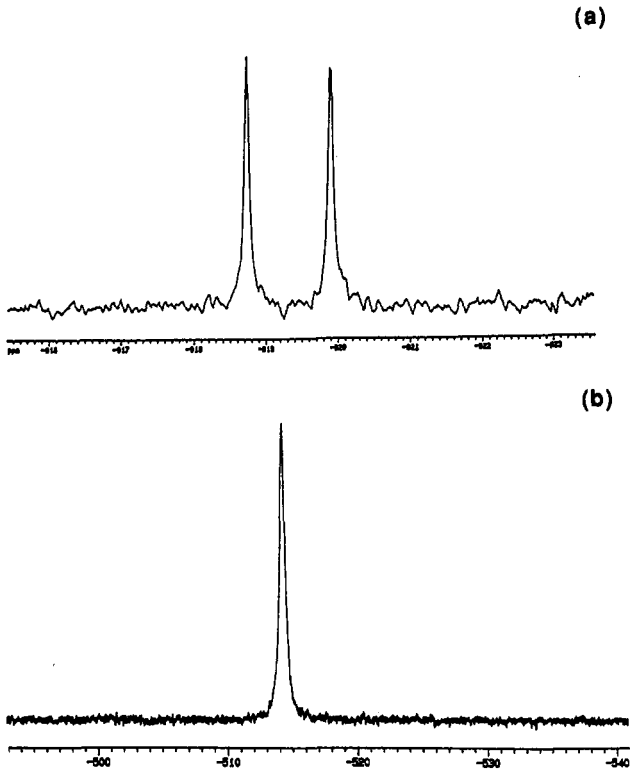

Figure 1. (a) ^{125}Te NMR spectrum of HTe^- in DMSO. (b) ^{77}Se NMR spectrum of HSe^- in MeOH. The Se–H coupling is not resolved.

recrystallized from, methanol. The solutions in methanol before and after crystallization gave rise to the characteristic doublet in the ^{125}Te solution NMR spectrum of HTe^-. The solid-state, proton-decoupled ^{125}Te and ^{123}Te NMR spectra of the solids yielded a single resonance, and the ^{125}Te chemical shifts are shown in Table I. No evidence of coupling to ^{125}Te was observed in the ^{123}Te spectra; we make this point here because in the spectrum of the $(Me_4N)_2Te_2$ product of the reaction of tellurium with Me_4NBH_4 the ^{123}Te–^{125}Te coupling was clearly resolved for the Te_2^{2-} ion.

The solids obtained gave solution and solid-state NMR spectra consistent with the presence of Et_4NTeH and *n*-Bu_4NTeH. Recrystallization of *n*-Bu_4NTeH from methanol appeared to give crystals suitable for study by X-ray diffraction. However, a completely satisfactory structural solution was not achieved.[9]

The only previous report of the isolation of a solid compound containing the TeH^- ion is the structural work of Huffman and Haushalter.[4] They were able to isolate crystals of Ph_4PTeH, suitable for an X-ray structure determination, by treating Ph_4PBr with the ethylenediamine extracts of solids with the nominal compositions K_2SiTe_3 and K_2GeTe_3. Since ethylenediamine was the only proton source in the system, it was surmised that the TeH^- ion was formed by aminolysis of the Si–Te or Ge–Te bond or by a reaction at the surface of the alloy. As already noted, solutions containing traces of TeH^- were obtained in the work of ref 2 by extracting K/Te alloys or the $LiPbTe_{0.67}Se_{0.33}$ alloy with ethylenediamine. The present work provides a simple and direct route to the synthesis of solutions containing TeH^- and to the isolation of the solids Et_4NTeH and *n*-Bu_4NTeH.

Given the difficulty experienced by Cusick and Dance[3] in characterizing the SeH^- ion formed by $NaBH_4$ reduction in ethanol/DMF solution and the apparent ease of formation of TeH^- compounds, samples of Me_4NSeH were prepared by reaction of Me_4NBH_4 with elemental selenium in DMF. A greenish-white compound was obtained, which was again soluble in methanol. The solution ^{77}Se NMR chemical shift was the same as that given in Table I for the reaction of $NaBH_4$ with selenium in methanol. The solid-state ^{77}Se NMR spectrum again yielded a single line, and $\delta(^{77}Se)$ for the solid is –465 ppm (Table I).

Crystals of Me_4NSeH were obtained on recrystallization from MeOH, and the crystal structure is reported below.

X-ray Crystal Structure of Me_4NSeH. Me_4NSeH was found to be isostructural with Me_4NBr,[10] which displays CsCl-like ionic packing. The atomic coordinates are given in Table II, and the unique set of bond distances and angles are listed in Table III. SeH^- lies on the crystallographic 4-fold axis, while N is on a $\bar{4}$ point. The closest interionic "contacts" are between Se and H(2) (3.12(4) Å) located in four symmetry-equivalent positions related to one another by the elements of the 4-fold rotation axis and to H(2) as given in Table III by the following transformations: $-x$, $1-y$, $-z$; $-^1/_2+y$, $-x$, $-z$; $^1/_2+x$, $-^1/_2+y$, $-z$; $1-y$, $^1/_2+x$, $-z$. The hydridic atom H(3) cannot be said to be unambiguously located. However, the feature we have associated with it is chemically reasonable and is consistent with the SeH^- ion having its center of mass on or near the 4-fold axis and either oscillating or being disordered between different orientations about this axis.

Table I. ^{125}Te and ^{77}Se Solution and Solid-State NMR Data[a]

		$\delta(^{125}Te)$, ppm	$^1J_{^{125}Te-^1H}$, Hz
TeH^-	DMSO soln	–919	160 ± 4
	DMF soln	–987	165 ± 4
	CH_3CN soln	–1060	160 ± 3
	C_2H_5OH soln	–1178	107 ± 3
	H_2O soln	–1249	97 ± 3
	MeOH soln	–1209	134 ● 4
n-Bu_4NTeH	solid	–876	
Et_4NTeH	solid	–970	
		$\delta(^{125}Te)$, ppm	$^1J_{^{125}Te-^{125}Te}$, Hz
$(Me_4N)_2Te_2$	solid	–880	3,568 ● 12
		$\delta(^{77}Se)$, ppm	$^1J_{^{77}Se-^1H}$, Hz
SeH^-	MeOH soln	–514	not resolved
Me_4NSeH	solid	–465	

[a] ^{125}Te chemical shifts are relative to Me_2Te, and those for ^{77}Se, relative to Me_2Se. Errors in measured peak positions are less than 1 ppm but are small compared to systematic errors arising from concentration and solvent dependence of the chemical shifts.

Table II. Fractional Atomic Coordinates (×10⁴) and Isotropic or Equivalent[a] Isotropic Temperature Factors (Å² × 10⁴) for Me_4NSeH

atom	*x*	*y*	*z*	*U*(iso)
Se	2500	2500	3653(1)	550[a]
N	2500	7500	0	341[a]
C	958(4)	7500	1544(5)	516[a]
H(1)	977(32)	8502(32)	2572(35)	662(60)
H(2)	16(49)	7500	619(52)	595(100)
H(3)	2500	2500	5955(244)	2277(968)

[a] The equivalent isotropic temperature factor is the cube root of the product of the principal axes of the ellipsoid.

Table III. Bond Distances and Angles for Me_4NSeH

Distances (Å)			
Se–H(3)	1.3(2)	N–C	1.496(4)
C–H(1)	0.98(3)	C–H(2)	0.91(4)
Angles (deg)			
C–N–C[a]	109.9(1)	C–N–C[b]	108.7(2)
H(1)–C–N	109(2)	H(2)–C–N	109(2)
H(1)–C–H(1)[c]	107(2)	H(2)–C–H(1)	111(2)

[a] $y-0.5$, $1-x$, $-z$. [b] $0.5-x$, $1.5-y$, z. [c] x, $1.5-y$, z.

(9) X-ray examination of a crystal of *n*-Bu_4NTeH at 236 K revealed a *C*-centered monoclinic unit cell of dimensions a = 14.568(4) Å, b = 14.452(4) Å, c = 19.767(2) Å, and β = 111.39(2)°. The $l = 2n+1$ data have an average intensity 0.05 times that of the $l = 2n$ data. A disordered model for the even-l data superstructure has been refined to R = 0.05 and is completely consistent with the formulation *n*-Bu_4NTeH (Z = 8). A satisfactory (nondisordered) model for the $l = 2n+1$ data has not been obtained.

(10) Wyckoff, R. W. G. *Z. Kristallogr.* **1927**, *67*, 91.

Preparation of $(Me_4N)_2Te_2$. In contrast to the reactions of Et_4NBH_4 and n-Bu_4NBH_4 in DMF with tellurium, which produced white TeH^- compounds, and the reaction of Me_4NBH_4 with Se, which gave a greenish-white solid, $(Me_4N)SeH$, the reaction of Me_4NBH_4 with tellurium produces a purple-blue solid. This solid dissolves in methanol to give an intense, deeply-red solution, characteristic of Te_3^{2-} or a higher polyanion. On removal of the methanol, the purple-blue solid is recovered. The methanol solution was found, surprisingly, to give a sharp, well-resolved doublet due to TeH^-, and no other tellurium resonance was observed in this solution.

The purple-blue compound gave a single resonance in the ^{125}Te solid-state NMR spectrum, but the ^{123}Te spectrum clearly showed the presence of Te–Te coupling, consistent with the presence of the Te_2^{2-} ion (Figure 2a). The $^1J_{^{125}Te-^{125}Te}$ coupling constant (Table I) calculated from the observed ^{123}Te spectrum is in reasonable agreement with that observed for the Te_2^{2-} ion in liquid ammonia by Bjorgvinsson and Schrobilgen[2] ($\delta = -1080$ ppm, $^1J_{^{123}Te-^{125}Te} = 3645$ Hz).

Crystals of the purple-blue compound were subjected to an X-ray crystal structure determination, and it was confirmed that the compound is indeed $(Me_4N)_2Te_2$.

The results of the experiments in which $(Me_4N)_2Te_2$ is dissolved in MeOH suggest that the Te_2^{2-} ion is unstable in solution, and the appearance of TeH^- as the dominant solution species in the NMR points to a disproportionation followed by the reaction of Te^{2-} with methanol. A possible scheme could be

$$2Te_2^{2-} \rightleftarrows Te^{2-} + \underset{\text{deep red}}{Te_3^{2-}}$$

$$Te^{2-} + MeOH \rightleftarrows TeH^- + MeO^-$$

The Te_3^{2-} ions must be involved in exchange and do not give rise to an observable ^{125}Te NMR resonance. On removal of the solvent, the above equilibria are reversed and $(Me_4N)_2Te_2$ crystallizes out, as confirmed by ^{123}Te solid-state NMR.

While the reaction of Me_4NBH_4 with tellurium gave excellent yields of $(Me_4N)_2Te_2$, reactions with Se gave only Me_4NSeH. All attempts to prepare $(Me_4N)_2Se_2$, for example by varying the solvent and temperature etc., were unsuccessful. The Se_2^{2-} ion is known to be relatively unstable in solution, and neither Cusick and Dance[3] nor Bjorgvinsson and Schrobilgen[2] were able to obtain solution NMR evidence for this species.

Attempts were made to prepare higher polyanions of tellurium by reacting $(Me_4N)_2Te_2$ with tellurium in DMF. Stoichiometric quantities of reactants were used which would, in principle, yield Te_3^{2-}, Te_4^{2-}, and Te_5^{2-}. In each case tellurium metal was observed to react with $(Me_4N)_2Te_2$ in DMF to form red solutions which, upon filtration and removal of the solvent at room temperature, yielded black solids. However, the solid-state NMR spectra of these residues showed multiple ^{125}Te resonances, indicating the presence of mixtures.

X-ray Crystal Structure of $(Me_4N)_2Te_2$. The structure of $(Me_4N)_2Te_2$ (Figure 3) represents a distortion of the anti-fluorite structure. Each Te_2^{2-} anion is centered on a $\bar{3}$ point and is surrounded by an approximate cube of Me_4N^+ cations distorted along the 3-fold axis. Alternate quasi-cubic interstices in the array of cations are occupied by anions. Each cation has one of its N–C bonds (C(1)) lying on a 3-fold axis and is surrounded by an approximate tetrahedron of anions opposite the N–C bonds. The atomic coordinates are given in Table IV, and the unique set of bond distances and angles are listed in Table V. The closest interionic "contacts" are between Te and H(22) (3.19(3) Å) and its 3-fold-rotation-related equivalents. There are similar "contacts" with symmetry equivalents of H(21) (3.21(4) Å), H(23) (3.31(4) Å), and H(1) (3.46(3) Å).

Early estimates of the bond length in ditelluride anions were made from X-ray powder diffraction on $MgTe_2$[5] (2.70(1) Å) and

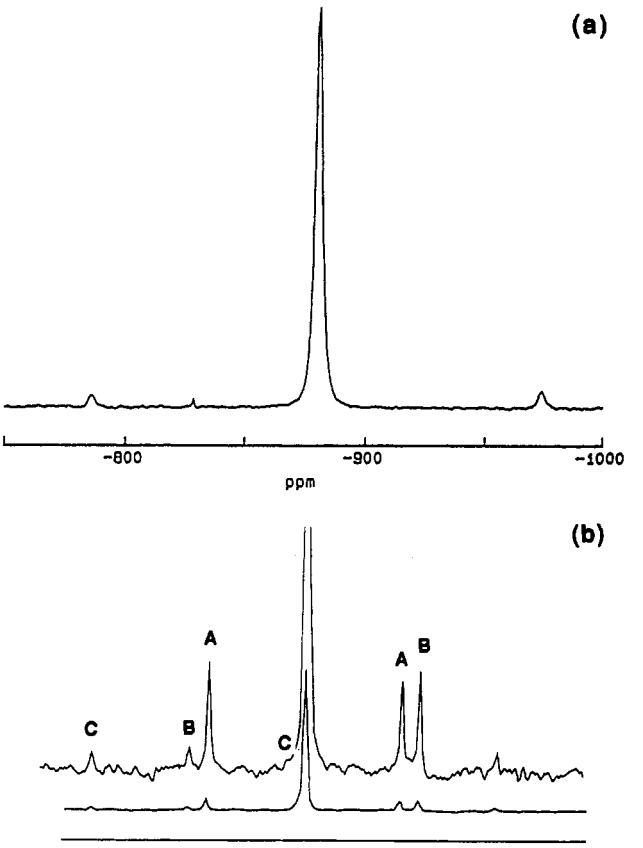

Figure 2. (a) Solid-state ^{123}Te NMR spectrum of $(Me_4N)_2Te_2$ at MAS of 3000 Hz showing the coupling to ^{125}Te. (b) Solid-state ^{123}Te NMR spectrum of $(Me_4N)_2Te_2$ at MAS of 1250 Hz showing (A) the spinning sidebands of the center line, (B) the J-coupled center bands, and (C) the spinning sidebands of peaks B.

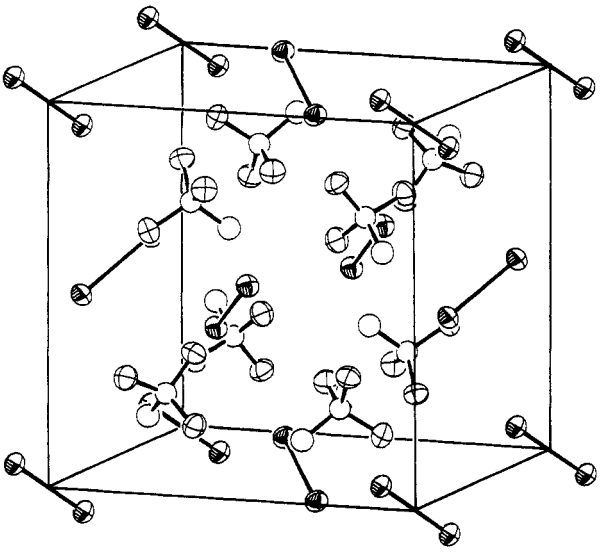

Figure 3. Unit cell of $(Me_4N)_2Te_2$.

from neutron diffraction on $MnTe_2$[6] (2.73(3) Å). In $(NMe_4)_2Te_2$, the Te–Te bond length (2.7371(6) Å) is significantly shorter than that recently reported[8] for the single-crystal X-ray structure of β-K_2Te_2 (2.790(1) Å) or the powder X-ray study of α-K_2Te_2 (2.86 Å), presumably as a consequence of reduced cation–anion interactions with the larger NMe_4^+ cation. A similar difference in Te–Te bond lengths was observed for the Te_3^{2-} anions in K_2Te_3[11] (2.805(5), 2.802(5) Å) and in $\{K\text{-}2,2,2\text{-crypt}\}_2Te_3\cdot en$[12] (2.720(4), 2.692(5) Å). For the higher polytellurides, Te_4^{2-} and Te_5^{2-}, in the absence of strong interionic interactions, the terminal Te–Te

(11) Eisenmann, B.; Schäfer, H. *Angew. Chem., Int. Ed. Engl.* **1978**, *17*, 684.
(12) Cisar, A.; Corbett, J. D. *Inorg. Chem.* **1977**, *16*, 632.

bond lengths are typically shorter (~2.70 Å) while the interior Te–Te bond lengths are slightly longer (~2.75 Å)[7] than that in $(NMe_4)_2Te_2$.

Solid-State NMR of $(Me_4N)_2Te_2$ and Me_4NSeH. As can be seen from Figure 2b, in the solid-state ^{123}Te NMR spectrum of $(Me_4N)_2Te_2$, the spinning sidebands of the two J-coupled satellites have completely different patterns of intensity. This phenomenon has been observed by Harris *et al.*[13] and explained as arising from the coupling anisotropy which adds to the chemical shift anisotropy for one satellite and subtracts for the other.

The derivation of resonance frequencies governed by anisotropic chemical shifts, J couplings, and dipolar couplings has been discussed by Zilm and Grant.[14] The present case is particularly simple, since the Te–Te bond lies along a crystallographic 3-fold axis, requiring the shielding and J-coupling tensors to be axially symmetric. The unique axes of these tensors must lie along the bond and be coincident with the unique axis of the dipolar coupling.

It has been pointed out[13] that there may be a sign inconsistency in ref 14. We therefore give the complete derivation for the simple axially symmetric AX case. We work entirely in frequency units and characterize the axially symmetric chemical shift by the parameters $\nu_\parallel$ and $\nu_\perp$, which represent the resonance frequency of an uncoupled spin with the field directed parallel and perpendicular, respectively, to the unique axis. We write ν_i for the isotropic resonance frequency and $\Delta\nu$ for $\nu_\parallel - \nu_\perp$. Similar notations are used for the components of the J and dipolar couplings. Thus, when the field makes an angle θ with the bond axis, the uncoupled resonance frequency is given by

$$\nu = \nu_i + {}^1/_3(3\cos^2\theta - 1)(\nu_\parallel - \nu_\perp) \quad (1)$$

similarly

$$J = J_i + {}^1/_3(3\cos^2\theta - 1)(J_\parallel - J_\perp) \quad (2)$$

and

$$\mathcal{D} = 0 + {}^1/_3(3\cos^2\theta - 1)(D_\parallel - D_\perp) \quad (3)$$

where

$$D_\perp = D \quad \text{and} \quad D_\parallel = -2D$$

with $D = \mu_0 h\gamma_A\gamma_X/16\pi^2 r^3$. Here μ_0 is the permeability of space, h is Planck's constant, γ_A and γ_X are the gyromagnetic ratios of the A and X nuclei, and r is the internuclear distance.

The two lines of the A spectrum have frequencies

$$\nu_+ = \nu_A - {}^1/_2(\mathcal{D} + J) \quad \text{for } m_X = +{}^1/_2$$

$$\nu_- = \nu_A + {}^1/_2(\mathcal{D} + J) \quad \text{for } m_X = -{}^1/_2$$

Thus substituting (1)–(3)

$$\nu_+ = \nu_{iA} - {}^1/_2J_i + {}^1/_3(3\cos^2\theta - 1)[\Delta\nu_A - {}^1/_2(\Delta J - 3D)] \quad (4)$$

$$\nu_- = \nu_{iA} + {}^1/_2J_i + {}^1/_3(3\cos^2\theta - 1)[\Delta\nu_A + {}^1/_2(\Delta J - 3D)] \quad (5)$$

If one performs a Herzfeld–Berger[15] analysis of the sideband intensities of an uncoupled line, the product of the rotor speed and the Herzfeld–Berger μ parameter yields the quantity $(\nu_\parallel - \nu_\perp)$. Thus by comparison of eq 1 with eqs 4 and 5, it can be seen that, by Herzfeld–Berger analysis of the sideband intensities of the J-coupling satellites, the square-bracketed terms in eqs 4 and 5 may be obtained. Since $\nu_\parallel - \nu_\perp$ may be found from analysis of the uncoupled center line and since D may be calculated from the X-ray bond length, ΔJ may be determined.

As pointed out by Harris et al.,[13] when $3D$ exceeds $|\Delta J|$, the sign of the coupling anisotropy is known, and hence the sign of J may be determined unambiguously by observation of which coupling satellite has the larger anisotropy. If this condition does not hold, an ambiguity as to the sign of J remains (see below).

Closer inspection of Figure 2b indicates that the low-frequency J-coupled line, which shows no spinning sidebands, is of appreciably greater intensity than the sum of centerband and sideband intensities for the high-frequency manifold. Indeed, using the Herzfeld–Berger calculation to estimate the intensities of sidebands that are below the noise level, we find that the high-frequency manifold has only 57% of the intensity of the low-frequency line. This must indicate a difference in the strength with which these lines are excited by cross-polarization. Studies of the cross-polarization dynamics of the uncoupled centerband showed that the intensity of this line is maximized with a contact time of 1.2 ms. Extending the contact leads to a decay in the signal (in the ^{125}Te spectrum), corresponding to a rotating frame relaxation time of 3.5 ms.

Thus it can be seen that the intensity is a delicate function of contact and relaxation times. If the high-frequency J-coupled line had a shorter rotating-frame relaxation time than its low-frequency partner, this intensity anomaly would be explained. If the Te_2^{2-} anion is undergoing a librational motion in the crystal, this is exactly what would be expected. The combined chemical shift and coupling anisotropy, discussed above, will act as a relaxation source, in the presence of angular motions. Because of the much larger total anisotropy of the high-frequency line, it will have the shorter relaxation time and hence the lower intensity under cross-polarization conditions.

To test this conjecture, we have repeated the experiment with a contact time of 500 μs. This allows less time for rotating-frame relaxation, at the cost of a weaker signal. In this case, we find that the high-frequency manifold has 92% of the intensity of the low-frequency line. This appears to substantiate the above suggestions.

Analysis of the sideband intensities of the uncoupled resonance shows that its $\Delta\nu$ value is −136 ± 4 ppm, or −2140 ± 60 Hz, for the ^{123}Te resonance. The low-frequency J-coupled line shows no spinning sidebands at the lowest spinning frequency studied,

Table IV. Fractional Atomic Coordinates (×10⁴) and Isotropic or Equivalent[a] Isotropic Temperature Factors (Å² × 10⁴) for $(Me_4N)_2Te_2$

atom	x	y	z	U(iso)
Te	687.1(1)	687.1(1)	687.1(1)	442[a]
N	2855(2)	2855(2)	2855(2)	421(8)
C(1)	3606(3)	3606(3)	3606(3)	482(12)
C(2)	3572(3)	2346(3)	1893(3)	526[a]
H(1)	4189(20)	3279(25)	3976(26)	494(81)
H(21)	4202(25)	1860(26)	2264(30)	650(54)
H(22)	3144(26)	1759(25)	1409(27)	650(54)
H(23)	3879(26)	2960(25)	1491(29)	650(54)

[a] The equivalent isotropic temperature factor is the cube root of the product of the principal axes of the ellipsoid.

Table V. Bond Distances and Angles for $(Me_4N)_2Te_2$

Distances (Å)			
Te–Te[a]	2.7371(6)	N–C(1)	1.496(6)
N–C(2)	1.498(3)	C(1)–H(1)	0.88(2)
C(2)–H(21)	1.01(3)	C(2)–H(22)	1.00(3)
C(2)–H(23)	0.92(3)		
Angles (deg)			
C(2)–N–C(1)	109.5(2)	C(2)–N–C(2)[b]	109.4(2)
H(1)–C(1)–N	118(2)	H(1)–C(1)–H(1)[b]	100(3)
H(21)–C(2)–N	107(2)	H(22)–C(2)–N	114(2)
H(22)–C(2)–H(21)	102(3)	H(23)–C(2)–N	106(2)
H(23)–C(2)–H(21)	111(3)	H(23)–C(2)–H(22)	115(3)

[a] −x, −y, −z. [b] y, z, x.

(13) Harris, R. K.; Packer, K. J.; Thayer, A. M. *J. Magn. Reson.* **1985**, *62*, 284–297.
(14) Zilm, K. W.; Grant, D. M. *J. Am. Chem. Soc.* **1981**, *103*, 2913–2922.
(15) Herzfeld, J.; Berger, A. E. *J. Chem. Phys.* **1980**, *73*, 6021–6030.

namely 875 Hz. The noise level is such that the sideband intensity can be definitely stated to be less than 10% of that of the centerband. From the Herzfeld–Berger calculation we thus find that this line has an anisotropy of less than 1450 Hz in magnitude. Analysis of sideband intensities of the high-frequency band, using the spectrum at 875 Hz and two independent spectra at 1250 Hz, gives an anisotropy of −4500 ± 300 Hz. Thus using eq 5, a value of −2360 ± 400 Hz is predicted for the quantity $^1/_2(\Delta J - 3D)$. Equation 4 in turn predicts a total anisotropy of +220 Hz for the low-frequency line, well within the limit established above. From the crystallographically determined Te–Te bond length, the dipolar coupling constant D between ^{123}Te and ^{125}Te is calculated to be 484 Hz. Thus, finally, we arrive at the result $\Delta J \equiv J_\parallel - J_\perp = -4270 \pm 800$ Hz.

Since, as mentioned above, D is not large enough to dominate the sign of the coupling anisotropy, we do not know the absolute sign of J. Our average value for the magnitude of the isotropic J coupling between ^{123}Te and ^{125}Te is 2960 ± 5 Hz. This could arise either as $J_i = 2960$ Hz, $J_\parallel = 110$ Hz, $J_\perp = 4380$ Hz or as $J_i = -2960$ Hz, $J_\parallel = -5810$ Hz, $J_\perp = -1540$ Hz.

These results are in keeping with a growing body of evidence[16] that J couplings among heavy elements can have substantial anisotropies. The analysis of these couplings solely in terms of the Fermi contact mechanism is therefore not appropriate.

The solid-state NMR investigation of Me_4NSeH revealed interesting motional properties. Observation of the ^{77}Se line in a static sample, without decoupling, at room temperature, showed a single, slightly asymmetric resonance, with a full width at half-height of 1800 Hz. Assuming that SeH^- has the same bond length as H_2Se (1.47 Å), the Se–H dipolar coupling is 7240 Hz, and the static spectrum might be expected to be a Pake pattern of this width, with broadening by the more distant methyl protons. Thus considerable motional averaging must be present. This is consistent with the short observed T_1 value for ^{77}Se in this compound, namely 800 ± 200 ms. When the static spectrum is observed with proton decoupling, a typical axially symmetric chemical shift powder pattern is observed. The width of this pattern is 920 Hz, or 80 ppm. Thus the motions leading to averaging of the Se–H dipolar interaction cannot be isotropic but must be constrained in such a way as to leave the average Se environment axially symmetric. These motions must also average the chemical shift anisotropy, and the anisotropy of a static SeH^- ion must be considerably in excess of the 80 ppm mentioned above.

^{125}Te Mössbauer Data. ^{125}Te Mössbauer spectra for K_2Te_2 and $(Me_4N)_2Te_2$ are illustrated in Figure 4, and the Mössbauer parameters are given in Table VI. Data are also presented for samples in the K/Te system prepared as indicated in Table VI and as described in the Experimental Section.

The spectrum of K_2Te was a single resonance, as expected, while K_2Te_2, prepared in a variety of ways, yielded a quadrupole-split doublet with Δ of ca. 9.7 mm s^{-1}, in good agreement with that observed for $(Me_4N)_2Te_2$. The compound Et_4NTeH yielded a doublet with a somewhat smaller splitting of 7.5 mm s^{-1}. All of the spectra had relatively narrow line widths ($\Gamma_{theor} = 5.02$ mm s^{-1}), and the doublets were well-resolved. There was no evidence for the presence of mixtures or of unreacted tellurium in the K/Te samples, for example.

The nuclear quadrupole coupling constants for $^{125}TeH^-$ and $^{125}Te_2^{2-}$ can be compared with those for $H^{127}I$ (1640 MHz) and $^{127}I_2$ (2238 MHz), respectively,[17] molecules with which they are isoelectronic. The coupling constants calculated from the Δ values are found to be 432 MHz for $^{125}TeH^-$ and 558 MHz for Te_2^{2-}. It follows that $e^2qQ(^{125}Te)/e^2qQgnd(^{127}I)$ is 0.26 for TeH^- and 0.25 for Te_2^{2-}. However, in I_2 there is an asymmetry parameter of 0.12 and η cannot be deduced from the ^{125}Te spectra; hence these ratios are only approximate. These values compare well with that previously reported for $e^2qQ(^{125}TeCN^-)/e^2qQgnd(^{127}ICN)$ of 0.21.[18]

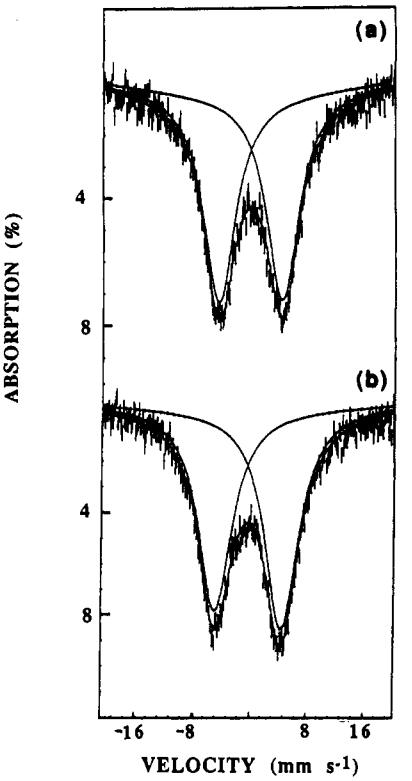

Figure 4. ^{125}Te Mössbauer spectra recorded at 4.2 K for (a) K_2Te_2 and (b) $(Me_4N)_2Te_2$.

Table VI. ^{125}Te Mössbauer Data Measured at 4.2 K

	δ,[a] mm s^{-1}	Δ,[b] mm s^{-1}	Γ,[c] mm s^{-1}
Te (metal)	0	7.5	6.5
K_2Te	0.54	0	5.9
K_2Te_2 (Te + K in $NH_{3(l)}$)	−0.43	9.6	5.9
K_2Te_2 (K_2Te + Te; 500 °C)	−0.46	9.8	6.5
K_2Te_2 (Te + K in en.)	−0.44	9.8	5.9
K_2Te_3 (2Te + 3K in en.)	−0.36	9.8	5.8
Et_4NTeH	−0.37	7.5	6.2
$(Me_4N)_2Te_2$	−0.44	9.7	5.9
$(PPN)_2Te_2$	−0.40	9.7	5.8

[a] With respect to Te metal (±0.08 mm s^{-1}). [b] Δ ± 0.1 mm s^{-1}. [c] Full width at half-maximum (±0.1 mm s^{-1}).

The quadrupole splitting of 9.7 mm s^{-1} for $(Me_4N)_2Te_2$ compares well with 7.7 mm s^{-1} reported[19] for $MnTe_2$, indicating the presence of considerable covalency in the latter.

In Table VI it can be seen that the sample prepared with the stoichiometry K_2Te_3 gave a spectrum essentially identical to that of K_2Te_2. This suggests that the terminal and bridging tellurium atoms in the bent Te_3^{2-} ion yielded overlapping absorptions which are indistinguishable from that of Te_2^{2-}. In a simple Townes–Dailey model[20] for quadrupole couplings, in Te_2^{2-} the tellurium will have a p-orbital imbalance $U_p \simeq +1$ while in Te_3^{2-} the central tellurium atom will have $U_p \simeq -1$ and the terminal atoms $U_p \simeq +1$. All three tellurium atoms should then yield similar quadrupole splittings, the difference in sign of the coupling constants being of no consequence in a quadrupolar doublet. Given that the range of isomer shifts for ^{125}Te is very small in comparison with that of the quadrupole splittings, the spectrum of Te_3^{2-} should comprise two closely overlapping doublets with a Δ value very similar to that of the doublet in Te_2^{2-}, as observed.

(16) Power, W. P.; Lumsden, M. D.; Wasylishen, R. E. *J. Am. Chem. Soc.* **1991**, *113*, 8257–8262.
(17) Perlow, G. J.; Perlow, M. R. *J. Chem. Phys.* **1966**, *45*, 2193.
(18) Jones, C. H. W.; Sharma, R. D. *Organometallics* **1987**, *6*, 1419.
(19) Pasternak, M.; Spijkervet, A. L. *Phys. Rev.* **1969**, *181*, 574.
(20) Das, T. P.; Hahn, E. L. *Nuclear Quadrupole Resonance Spectroscopy*; Supplement 1 of Solid State Physics; Academic Press Inc.: New York, 1958.

Experimental Section

Synthesis. All samples were prepared using freshly-distilled, oxygen-free solvents, and all manipulations were carried out under oxygen-free nitrogen.

Solutions of TeH^- were prepared in various solvents by reducing tellurium metal with a stoichiometric quantity of $NaBH_4$. With stirring, the reaction was smooth and rapid and the solutions were quite stable in the absence of oxygen. The solutions were filtered prior to the acquisition of their NMR spectra.

In recent work[21] the reaction of $NaBH_4$ with selenium has been studied in triglyme and diglyme and ^{11}B NMR evidence found for the presence of $[H_3B–Se–Se–BH_3]^{2-}$, from which $Cs_2[(BH_2)_6Se_4]$·CsBr was prepared. In the reaction of selenium or tellurium with $NaBH_4$ in $THF·BH_3$, $[H_3B–\mu_2\text{-}E(B_2H_5)]^-$ peaks were observed in the ^{11}B NMR spectra. In the present work, no evidence was found for the formation of chalcogen–boron adducts. For reactions in DMF, for example, the ^{11}B NMR spectra only gave evidence for the formation of $H_3B·N(CH_3)_3$ ($\delta(^{11}B) = 28.5$ (q), with respect to BH_4^-, $^1J_{^{11}B-^1H} = 91.5$ Hz), which has been characterized previously as a product of the reaction of $LiBH_4$ with DMF.[22]

For the preparation of n-Bu_4NTeH, Et_4NTeH, and Me_4NSeH, the appropriate R_4NBH_4 compound was reacted with tellurium or selenium in DMF. The solution was filtered, the solvent removed, and the solid product recrystallized from acetonitrile as white or yellowish-white compounds.

Upon reaction of Me_4NBH_4 with tellurium in DMF, purple-blue $(Me_4N)_2Te_2$ precipitated and the residual solution showed only the presence of TeH^- in the ^{125}Te NMR. The solid was recrystallized from methanol as plates. The sample of $(PPN)_2Te_2$, PPN = $(Ph_3P)_2N^+$, was prepared by reacting $(PPN)BH_4$ with tellurium in DMF.

The reactions of potassium with tellurium in the appropriate quantities to yield the stoichiometries K_2Te, K_2Te_2, K_2Te_3, and K_2Te_4 were carried out in ethylenediamine, followed by removal of the solvent. A sample of K_2Te_2 was also prepared by reaction in liquid ammonia, while another sample was prepared by reacting K_2Te with the stoichiometric quantity of tellurium in an evacuated quartz ampule at 500 °C. All manipulations were again carried out in an oxygen-free atmosphere.

The ^{125}Te NMR spectra of K_2Te, K_2Te_2, K_2Te_3, and K_2Te_4 were obtained in ethylenediamine at ambient temperature. While K_2Te yielded a narrow single line ($\delta = -1388$ ppm), the other samples gave broadened single lines of increasingly positive chemical shift: K_2Te_2, $\delta = -1028$ ppm; K_2Te_3, $\delta = -416$ ppm; K_2Te_4, $\delta = -118$ ppm. The broad line widths were a consequence of exchange occurring in solution, and the shifts show the same trend as, but are not in exact agreement with, those of Bjorgvinsson and Schrobilgen.[2] The latter reference should be consulted for a detailed study of this system.

Crystallography. All crystals were mounted under argon atmosphere and sealed in Lindeman capillary tubes. Data were recorded at ambient temperature (297 K) for Me_4NSeH and $(Me_4N)_2Te_2$ on an Enraf-Nonius CAD4F diffractometer using graphite-monochromatized Mo Kα radiation. Unit cell dimensions were determined from 25 well-centered reflections ($37° \le 2\theta \le 42°$ for Me_4NSeH; $40° \le 2\theta \le 46°$ for $(Me_4N)_2Te_2$). Two intensity standards measured every hour of exposure time showed no systematic variations during the course of data acquisition for Me_4NSeH and declined by 2% for $(Me_4N)_2Te_2$. The data were corrected for the effects of absorption using the Gaussian integration method. The corrections were checked versus ψ-scan measurements. Data reduction included corrections for intensity-scale variation and for Lorentz and polarization effects.

The structure of Me_4NSeH was solved by analogy with that of Me_4NBr.[7] After refinement of Se, N, and C (all anisotropic) and H(1) and H(2) (isotropic), a difference map with only data for which $((\sin\theta)/\lambda)^2 \le 0.15$ Å^{-2} showed a broad region of positive electron density with a maximum of 0.15(4) e Å^{-3} occurring at 1.54 Å from Se and on the 4-fold axis. H(3) was placed in this position, and its z coordinate and isotropic temperature factor were included in the refinement. The final full-matrix least-squares refinement of 21 parameters, using 180 reflections ($I_o \ge 2.5\sigma(I_o)$), included anisotropic thermal parameters for all non-hydrogen atoms and independent isotropic thermal parameters for the hydrogen atoms.

The structure of $(Me_4N)_2Te_2$ was solved by analogy with that of $N_2H_6Cl_2$.[23] The final full-matrix least-squares refinement of 32 parameters, using 454 reflections, included an extinction parameter,[24] anisotropic thermal parameters for Te and C(2), and independent isotropic thermal parameters for N, C(1), and H(1). A single parameter was refined for the isotropic thermal motion of H(21)–H(23).

Empirical weighting schemes based on counting statistics were applied such that $\langle w(|F_o| - |F_c|)^2\rangle$ was nearly constant as a function of both $|F_o|$ and $(\sin\theta)/\lambda$. The programs used for absorption corrections, data reduction, structure solution, initial refinement, and plot generation were from the NRCVAX Crystal Structure System.[25] The program suite CRYSTALS[26] was used for final the refinements. Complex scattering factors for neutral atoms[27] were used in the calculation of structure factors. All computations were carried out on a MicroVAX-II computer. Crystal and refinement data are given in Table VII.

Table VII. Crystallographic Data for the Structure Determinations of $(Me_4N)_2Te_2$ and Me_4NSeH

formula	$Te_2N_2C_8H_{24}$	$SeNC_4H_{13}$
fw	403.49	154.11
crystal system	cubic	Tetragonal
space group	$Pa\bar{3}$	P4/nmm
a, Å	11.499(1)	7.8855(8)
c, Å		5.6484(5)
V, Å^3	1520.5	351.22
Z	4	2
ρ_c, g cm^{-3}	1.763	1.457
λ(Mo, Kα_1), Å	0.709 30	0.709 30
μ(Mo Kα), cm^{-1}	38.2	51.8
min–max 2θ°	3–55	5–50
transm	0.382–0.570	0.241–0.447
$R(F)$[a]	0.018	0.020
$R_w(F)$[b]	0.020[c]	0.029[d]

[a] $R(F) = \sum||F_o| - |F_c||/\sum|F_o|$, for reflections having $I_o \ge 2.5\sigma(I_o)$. [b] $R_w(F) = [\sum(w(|F_o| - |F_c|)^2)/\sum(wF_o^2)]^{1/2}$, for reflections having $I_o \ge 2.5\sigma(I_o)$. [c] $w = [\sigma^2(F_o) + 0.00001F_o^2]^{-1}$. [d] $w = [\sigma^2(F_o) + 0.0002F_o^2]^{-1}$.

NMR Spectroscopy. Solution NMR spectra were obtained at ambient temperature on a Bruker WM-400 spectrometer at 126.1116 MHz for ^{125}Te and 76.1817 MHz for ^{77}Se. The solutions were contained over oxygen-free nitrogen in sealed tubes.

Solid-state spectra were recorded on the instrument previously described.[28] This gives resonance frequencies of 11.4 and 18.9 MHz for ^{77}Se and ^{125}Te, respectively. Chemical shifts were measured relative to external samples of H_2SeO_3 and $(PhTe)_2$. The secondary references were measured in our laboratory relative to $(CH_3)_2Se$ and $(CH_3)_2Te$ to convert shifts to the standard scales.

^{125}Te Mössbauer Spectroscopy. The ^{125}Te Mössbauer spectra were recorded using a constant-acceleration Harwell Instruments spectrometer with the ^{125}Sb/Cu source and the absorbers immersed in liquid helium, as previously described.[29] Absorbers, containing ca. 100 mg of naturally abundant tellurium, were mounted in Teflon holders in oxygen-free nitrogen, and the cross-sectional area of the samples was 2 cm^2. The samples were stored in liquid nitrogen prior to the spectra being recorded. Spectra were computer-fitted to independent Lorentzians, and the isomer shifts are quoted with respect to tellurium metal as a reference.

Acknowledgment. The authors wish to acknowledge grants in support of this work from the Natural Sciences and Engineering Research Council of Canada.

Supplementary Material Available: Tables of additional crystallographic experimental and structure refinement data and anisotropic thermal parameters (1 page). Ordering information is given on any current masthead page.

(21) Binder, H.; Loos, H.; Dermentzis, K.; Borrmann, H.; Simon, A. *Chem. Ber.* **1991**, *124*, 427.
(22) Linti, G.; Nöth, H.; Thomann, M. *Z. Naturforsch.* **1990**, *45B*, 1463.
(23) Donohue, J.; Lipscomb, W. N. *J. Chem. Phys.* **1947**, *15*, 115.
(24) Larson, A. C. *Crystallographic Computing*; Ahmed, F. R., Ed.; Munksgaard: Copenhagen, 1970; p 291.
(25) Gabe, E. J.; LePage, Y.; Charland, J.-P.; Lee, F. L.; White, P. S. NRCVAX—An Interactive Program System for Structure Analysis. *J. Appl. Crystallogr.* **1989**, *22*, 384.
(26) Watkin, D. J.; Carruthers, J. R.; Betteridge, P. W. CRYSTALS. Chemical Crystallography Laboratory, University of Oxford, Oxford, England, 1984.
(27) *International Tables for X-ray Crystallography*; Kynoch Press: Birmingham, England, 1975; Vol. IV, p 99.
(28) Gay, I. D.; Jones, C. H. W.; Sharma, R. D. *J. Magn. Reson.* **1989**, *84*, 501–504.
(29) Jones, C. H. W.; Sharma, R. D. *Organometallics* **1986**, *5*, 805.